

RADIATION MONITORING OF THE GEM MUON DETECTORS AT CMS

L. Dimitrov, P. Iaydjiev, G. Mitev, I. Vankov¹

Institute for Nuclear Research and Nuclear Energy, Bulgarian Academy of Sciences, Sofia

The higher energy and luminosity of future High Luminosity (HL) LHC determine a significant increasing of the radiation background around the CMS subdetectors, and especially in the higher pseudorapidity region. Under such heavy conditions, the RPC (used in muon trigger) most probably could not operate effectively. GEM (Gas Electron Multiplier) detectors have been identified as a suitable technology to operate in the high radiation environment in that region and test at CMS will start in 2016.

A monitoring system to control the absorbed radiation dose by the GEM under test is developed. Two types of sensors are used in it: RadFETs for total absorbed dose and p-i-n diodes for particle (proton and neutron) detection. The basic detector unit, called RADMON, contains two sensors of each type and can be installed at each GEM detector. The system has a modular structure, permitting one to increase easily the number of controlled RADMONs: one module controls up to 12 RADMONs, organized in three groups of four and communicates outside by RS 485 and CANBUS interfaces.

PACS: 29.40.Wk; 29.85.Ca

INTRODUCTION

The increasing of the energy and luminosity during the coming upgrades of CERN LHC creates more hostile environment for the detector used. In CMS especially the most heavy conditions will be created in the forward region of the muon system (with pseudorapidity η : $1.6 < \eta < 2.4$), where for the high-luminosity phase of the LHC one expects particle rates of several kHz/cm². This imposes severe restriction on the technology that can be used. The presently installed Bakelite-based RPCs in the $\eta < 1.6$ region are, for example, not able to sustain such rates.

To solve the problem CMS decided [1] to investigate the possibilities of the so-called GEM detectors. They are [2, 3] Micro-Pattern Gaseous Detectors that feature 50–100 μm spatial resolution, 4–5 ns time resolution, high detection efficiency, and proven high-rate capability and resilience against aging effects. The very high time and spatial resolution enable their simultaneous application for triggering and tracking information. After numerous tests [4, 5], first prototype of real CMS GEM detector is under production. Called GEM superchamber [6], it is composed of two chambers, mounted face to face at a distance of 20 mm.

¹E-mail: Ivan.Vankov@cern.ch

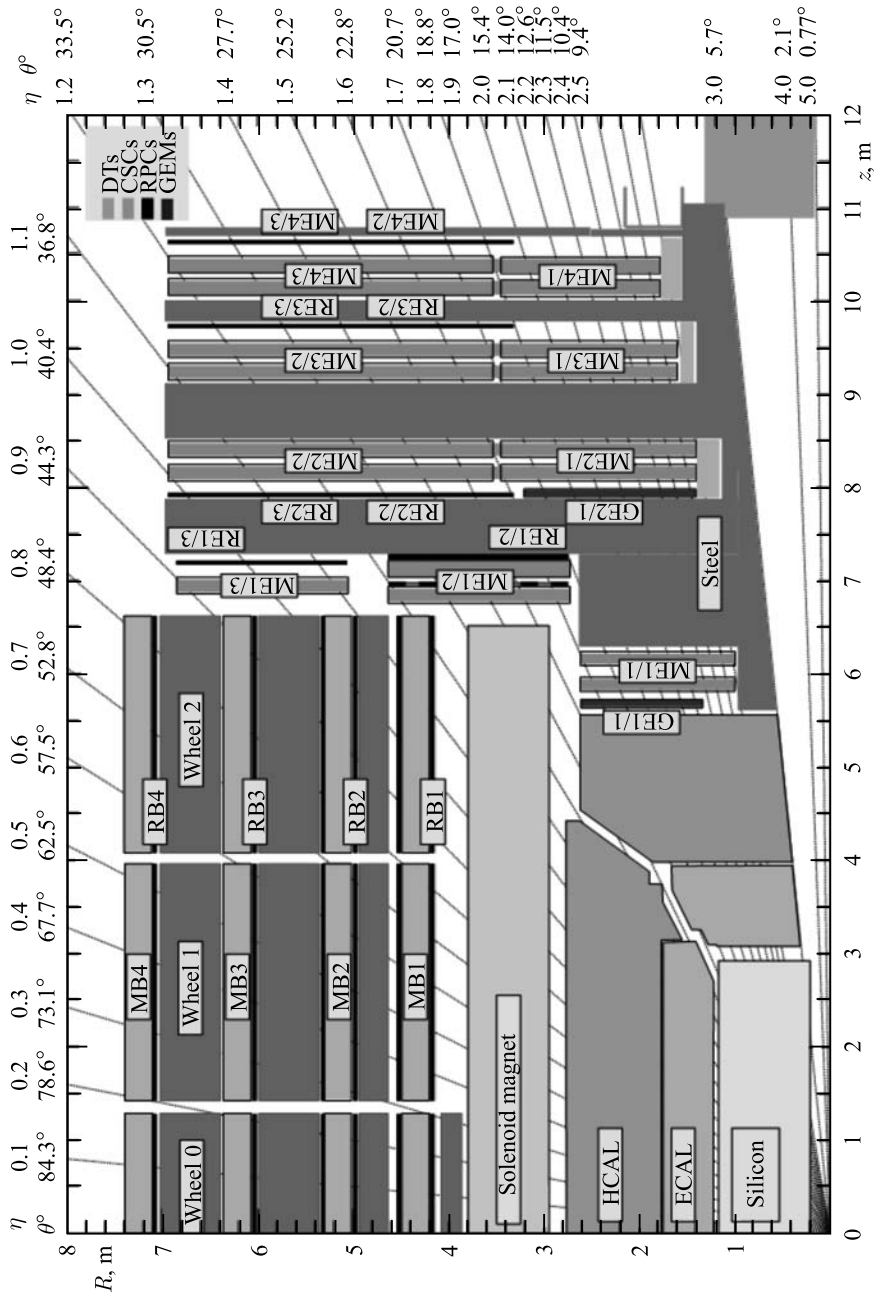


Fig. 1. Transverse section of the CMS detector showing the present muon system including RPCs, DTs and CSCs. The proposed locations for the GEM detectors in the two inner endcap stations are indicated as GE1/1 and GE2/1

The CMS program [7] foresees to equip each of the presently vacant insertion slots in inner endcap stations ($1.6 < \eta < 2.2$, Fig. 1) with 36 super GEMs. The installation in the first of them (labeled GE1/1) will be during the second LHC Long Shutdown in 2017–2018 and in the second one (labeled GE2/1) — during the third LHC Long Shutdown scheduled beyond 2020. For a first test only 4 superchambers will be installed in GE 1/1 station during the 2016–2017 LHC Year-end Technical Stop.

A control system for quantitative measurement of the dose, deposited in the GEMs during their operation at CMS, is developed and will be described in this paper.

1. SENSORS

A mixed radiation field composed of neutrons, photons and charged hadrons due to particles generated by the proton–proton collisions and reaction products of these particles with the sub-detector material of the experiment itself can be expected around the GEM chambers at CMS. A universal dosimetry device, called RADMON, is developed and produced at CERN for similar investigations [8, 9]. Different combinations of semiconductor radiation detectors can be installed in it.

For our purpose, we would like to use the usual configuration of two RadFETs and two p-i-n diodes. RadFETs [9, 10] measure the ionizing energy deposition (the creation of electron–hole pairs in the material) by the build-up of positive charge in the gate oxide layer and therefore give data about total absorbed dose. The positive trapped charge can be retained for long periods at room temperature, leading to a shift of the transistor’s gate threshold voltage V_{th} . It is measured as the voltage drop on the RadFET, when a constant drain-source current ($I_{ds} = i_{bias}$, Fig. 2) passes through the device.

The relation between the gate threshold voltage shift ΔV_{th} and the radiation dose D is strongly dependent on the electric field in the oxide during irradiation and on the RadFET process parameters, especially the thickness of the gate oxide. It is nonlinear and best approximated by $\Delta V_{th} = a \times D^b$ [9]. The coefficients a and b have to be determined during a calibration run under the same conditions as the measurement runs.

Both RadFETs used have different gate oxide thickness (t_{ox}) and therefore cover different dose ranges [11]: LAAS 1600 ($t_{ox} = 1.6 \mu\text{m}$) — $10^{-3} \cdot 10 \text{ Gy}$; REM 250 ($t_{ox} = 0.25 \mu\text{m}$) — 0.1 Gy to tens of kGy. Their combination provides a wide enough range of measured doses.

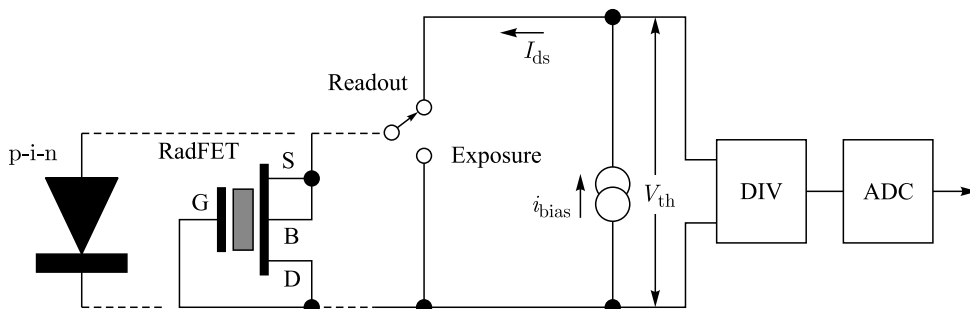


Fig. 2. Circuit of RadFET’s V_{th} or p-i-n VD readout

The p-i-n diodes are used only for particle's dose control: the particle interactions with the silicon intrinsic base produce defects, which decrease its conductivity. The main dependence between the base resistivity (ρ) and particle flux (Φ) is [10] $\rho = \rho_0 e^{\Phi/K\rho}$, where ρ_0 is the initial resistivity and $K\rho$ is a silicon material depending constant. It increases with the length of the silicon base and its initial resistivity. The dose output signal is received by measuring the diode's voltage V_D when forcing a constant bias current pulse in forward direction, i.e., using the circuit of Fig.2 with a diode at the place of the RadFET. In both cases, the accumulated dose corresponds to the difference between the final and initial value of the voltage (ΔV_{th} or ΔV_D).

Both p-i-n diodes used are also of different sensitivity: CMRP (base length 1 mm, $\rho_0 \approx 10 \text{ k}\Omega \cdot \text{cm}$) — $\Phi = 10^8 - 2 \cdot 10^{12} \text{ cm}^{-2}$; BPW34 (base length 210 μm , $\rho_0 \approx 2.5 \text{ k}\Omega \cdot \text{cm}$) — $\Phi = 2 \cdot 10^{12} - 4 \cdot 10^{14} \text{ cm}^{-2}$.

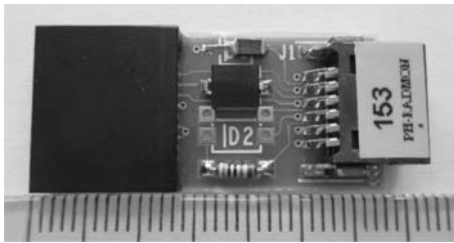


Fig. 3. RADMON PCB

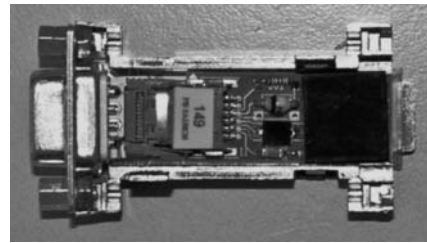


Fig. 4. Inside view of a RADMON box

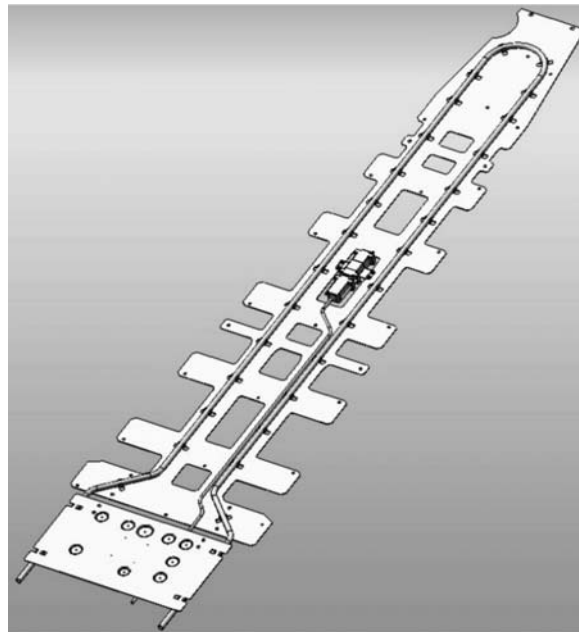


Fig. 5. RADMON box at a GEM cooling plate

A thermistor is also installed on the RADMON PCB (Fig. 3) because the both reading-out voltages (V_{th} and V_D) are dependent on the temperature. The thermistor's resistance is measured in the same manner as the sensor's voltages and the readout temperature can be used for data correction to increase the accuracy.

For our purpose the RADMON is put in a plastic box (Fig. 4), which is installed in the center of GEM cooling plate (Fig. 5) and is connected by a cable to the camera patch-panel.

2. RADMON CONTROL AND READOUT SYSTEM

The block diagram of the control and readout system (Fig. 6) is very similar to that developed by us for the control of the radiation doses at CERN GIF++ [12]. The Main Controller unit is managed by a microcontroller, PIC24HJ64 GP504, and contains three RADMON nodes. Up to four RADMONs can be connected to one node (through a passive splitter). The difference is due to the increased number of radiation sensors in each RADMON — 4 instead of 2. Thus, the number of the wires to each unit becomes 6 (to 4 sensors, 1 thermistor and ground) and the number of addresses in each node reaches 24 (5-line bus).

The four different types of sensors require individual readout currents. Their values are selected to provide a minimum temperature dependence of the measured voltage (V_{th} , V_D). They are generated by the PIC and fed to a DAC, whose output voltage (U_{curr_set} , Fig. 6) controls the RadFET's individual voltage-to-current converters (V/I) as is shown in Fig. 7. At high doses, the V_{th} value can reach relatively high voltages (more than 30 V). For this

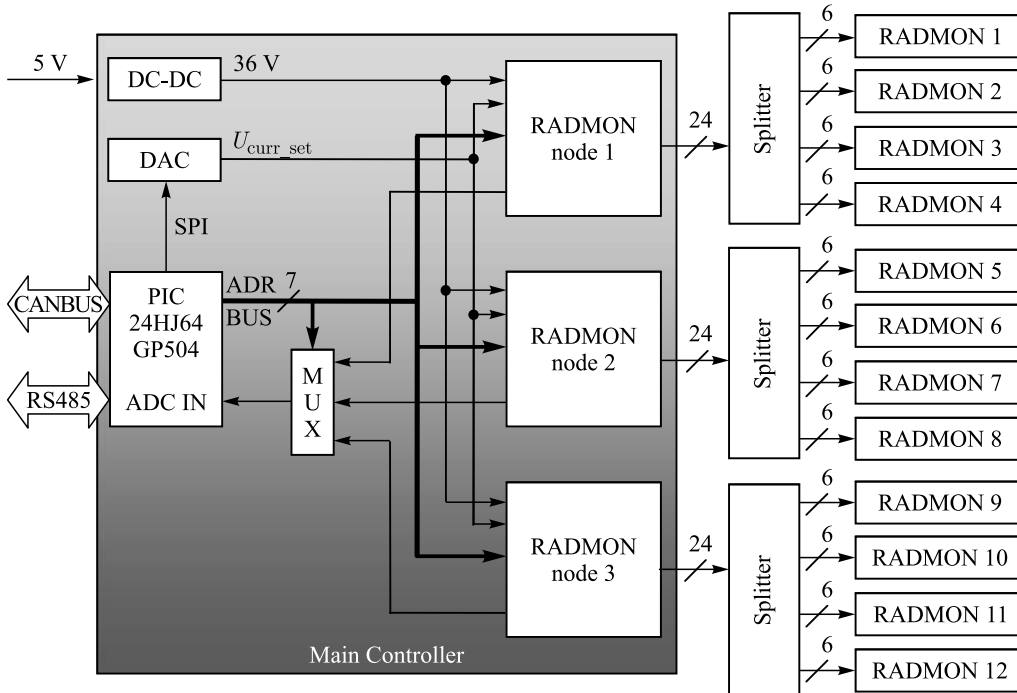


Fig. 6. Block diagram of the RADMON control and readout system

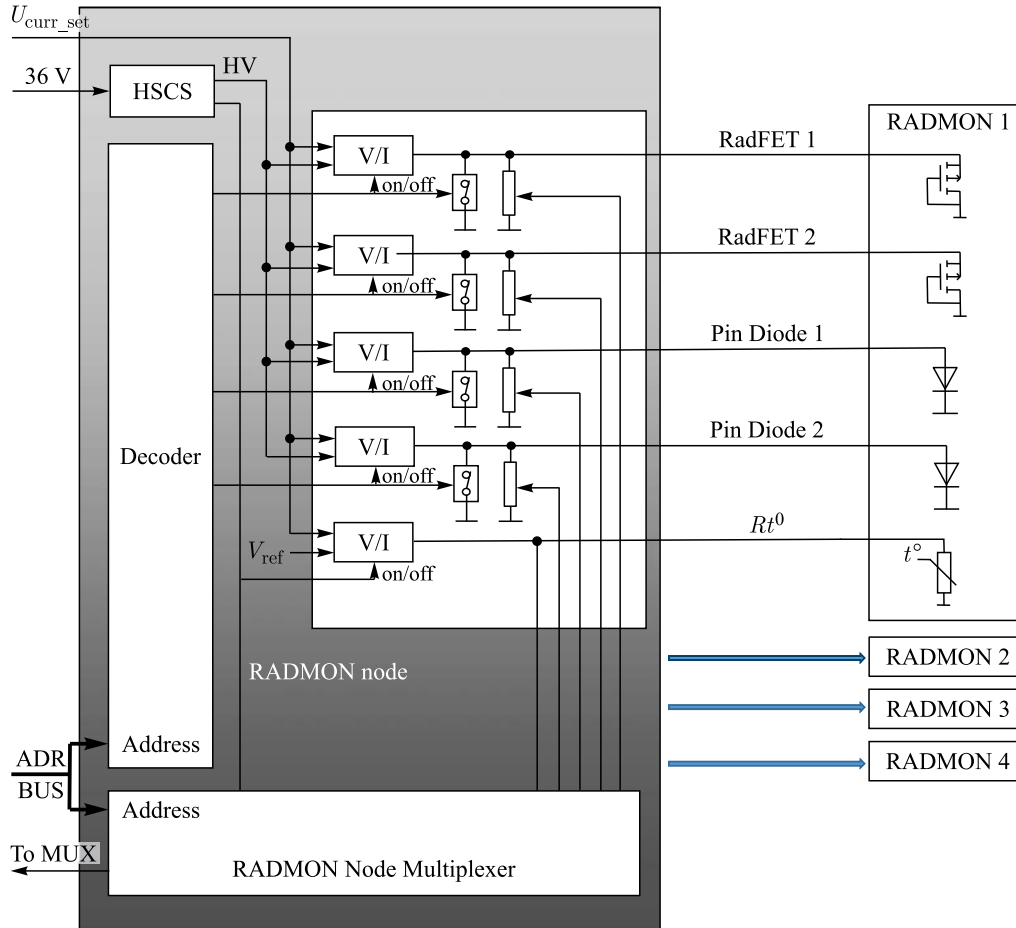


Fig. 7. Block diagram of the RADMON node. HSCS — high side current sensor; V/I — voltage-to-current converter

reason, an onboard DC-DC converter (Fig. 6) provides 36 V for the normal operation of the V/I converters.

The current is fed to the radiation sensors only for a short period of time to read the accumulated dose value. During the rest of the time all pins are grounded and the bias current is zero. A decoder (Fig. 7) selects which V/I converter should be active and opens the corresponding grounding switch to allow measurement. The reading of the thermistor value follows the same procedure but no grounding of its electrodes is necessary. The read voltages are scaled down and fed to the RADMON node multiplexer. It selects which of the outputs will be fed to the PIC ADC multiplexer (MUX, Fig. 6). The minimum time at which the channels can be scanned is limited by sensor's requirement and is about 30 s for all the three nodes.

The main controller has to be connected to an external DAQ system over a CANBUS or an RS485 interface and can be powered over any of the interface lines or by installing the

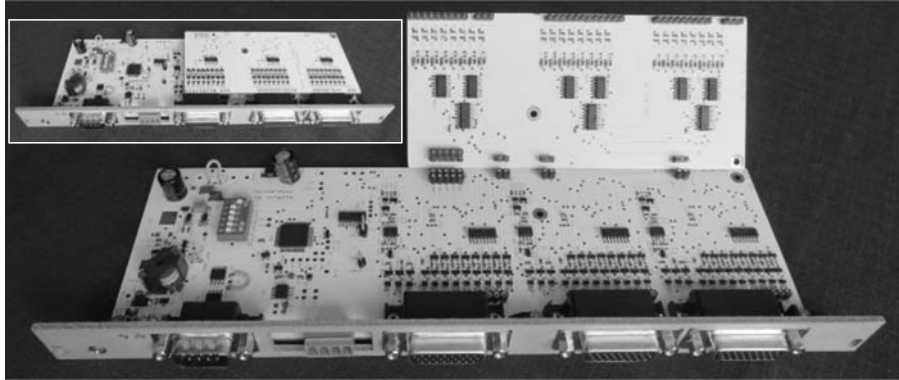


Fig. 8. Mechanical design of the RADMON control and readout system

PCB in a 6U Euro-standard crate. It can operate in single or multiple measurement modes. The main controller can store only limited data so the monitoring DAQ system has to read it periodically to prevent losses. The maximum time of the controller autonomous operation is inversely proportional to the number of connected RADMONs and the sampling rate.

A master–slave message based protocol is used. The DAQ system is the master. It can address one of several connected main controllers of this type. The address of each controller is the same both on CANBUS and on RS485 interfaces and is set by onboard micro-switches (Fig. 8).

The command set consists of messages for selecting a slave device, setting and reading operational parameters like system time and sampling rate, start and stop of the measurement and request for data. In case a controller remains constantly selected, it can be set to report automatically the data: either after every sample (when the measurement is completed) or when its data buffer is full.

CONCLUSIONS

A universal system for irradiation control is developed and built. First intended for radiation dose of the CMS muon GEM detectors measuring, it can be used for photon and particle radiation control at different places and objects of interest.

Acknowledgements. The “Radiation Monitoring of the GEM Muon Detectors at CMS” is a part of the “CMS Muon Endcap GEM Upgrade” project, which is financed by the Bulgarian Scientific Fund at the Ministry of Education and Science, grant DCERN 01/2 28.11.2013. Part of the radiation monitor system was designed under EC grant AIDA2020 No. 654168.

REFERENCES

1. *Abbaneo D. et al.* Characterization of GEM Detectors for Application in the CMS Muon Detection System // IEEE Nucl. Sci. Symp. Conf. Rec. 2010. P. 1416; RD51-Note-2010-005; arXiv:1012.3675.
2. *Sauli F.* GEM: A New Concept for Electron Amplification in Gas Detectors // Nucl. Instr. Meth. A. 1997. V. 386. P. 531.

3. *Cardini A., Bencivenni G., De Simone P.* The Operational Experience of the Triple-GEM Detectors of the LHCb Muon System: Summary of 2 Years of Data Taking // IEEE Nucl. Sci. Symp. Conf. Rec. 2012. P. 759.
4. *Abbateo D. et al.* Construction of the First Full-Size GEM-Based Prototype for the CMS High-*h* Muon System // IEEE Nucl. Sci. Symp. Conf. Rec. 2010. P. 1909; RD51-Note-2010-008; arXiv:1012.1524.
5. *Tytgat M. et al.* Construction and Performance of Large-Area Triple-GEM Prototypes for Future Upgrades of the CMS Forward Muon System // IEEE Nucl. Sci. Symp. Conf. Rec. 2011. P. 1019; RD51-Note-2011-012; arXiv:1111.7249.
6. *Abbateo D. et al. (CMS GEM Collab.)*. Status of the Triple-GEM Project for the Upgrade of the CMS Muon System // 3rd Intern. Conf. on Micro Pattern Gaseous Detectors, Zaragoza, Spain, July 1–6, 2013.
7. CMS Technical Design Report for the Muon Endcap. CERN-LHCC-2015-NNN, CMS-TDR-MMM. Draft V04-00. 2014.
8. *Ravotti F. et al.* Conception of an Integrated Sensor for the Radiation Monitoring of the CMS Experiment at the Large Hadron Collider // IEEE Trans. Nucl. Sci. 2004. V. 51, No. 6. P. 3642.
9. *Ravotti F. et al.* Radiation Monitoring in Mixed Environments at CERN: From the IRRAD6 Facility to the LHC Experiments // RADECS 2006 Workshop, Athens, Sept. 27–29, 2006. Paper PH-2 145.
10. *Ravotti F.* Development and Characterization of Radiation Monitoring Sensors for the High Energy Physics Experiments of the CERN LHC Accelerator. PhD Thesis. Montpellier Univ., France, 2006.
11. *Ravotti F., Glaser M., Moll M.* CERN Sensor Catalogue. TS-Note-2005-002. <https://edms.cern.ch/document/590497/1>.
12. *Dimitrov L. et al.* Radiation Monitoring at the New GIF++ Irradiation Facility at CERN // Bulg. J. Phys. 2015. V. 42, No. 2. P. 163.